Exact results for first-passage-time statistics in biased quenched trap models

Takuma Akimoto[1,*] and Keiji Saito[2]

[1]*Department of Physics, Tokyo University of Science, Noda, Chiba 278-8510, Japan*
[2]*Department of Physics, Keio University, Yokohama 223-8522, Japan*

We provide exact results for the mean and variance of first-passage times (FPTs) of making a directed revolution in the presence of a bias in heterogeneous quenched environments where the disorder is expressed by random traps on a ring with period L. FPT statistics are crucially affected by the disorder realization. In the large-L limit, we obtain exact formulas for the FPT statistics, which are described by the sample mean and variance for waiting times of periodically arranged traps. Furthermore, we find that these formulas are still useful for nonperiodic heterogeneous environments; i.e., the results are valid for almost all disorder realizations. Our findings are fundamentally important for the application of FPT to estimate diffusivity of a heterogeneous environment under a bias.

I. INTRODUCTION

Encountering a reactive molecule or finding a reactive site by a molecule is the first step in chemical reactions. Therefore, finding a specific target in stochastic processes is a fundamental problem in the context of chemical as well as biological reactions [1]. In particular, this target-search problem attracts significant interest in biomolecular reactions in cells such as transcription factors searching for a specific DNA sequence [2–4]. Many stochastic models have been utilized to unravel how biomolecules can efficiently reach the targets in cells [5–8], where a combination of three-dimensional (3D) free diffusion and one-dimensional (1D) sliding motion on DNA plays a vital role in reducing the first-passage time (FPT) to the target.

The 1D sliding motion is crucially affected by interactions between a searching molecule and DNA sequences [9]. DNA sequences exhibit anomalous fluctuations, such as long correlations and $1/f$ fluctuations [10]. Thus, a 1D sliding motion on DNA is described according to the diffusion in a quenched heterogeneous environment. In experiments, the diffusion coefficients of a repressor protein diffusing on DNA are obtained by single-particle-tracking measurements and show large trajectory-to-trajectory fluctuations [11,12]. These fluctuations are evidence of the heterogeneity of the environment. In fact, intrinsic fluctuations of the diffusion coefficients are observed in diffusion on heterogeneous environments such as the quenched trap model (QTM), which represents a random walk (RW) on a random energy landscape, and an annealed model of the QTM, which presents continuous-time RW (CTRW) [13,14].

The FPT statistics in heterogeneous environments are key quantities in target-search problems [15,16] and play an important role in estimating the diffusion coefficient [17]. In higher dimensions, the CTRW provides a good description of diffusion in quenched heterogeneous environments, and hence the FPT statistics with the CTRW have been intensively studied [18–21]. However, in 1D systems, the diffusion in quenched potentials cannot be approximated with the CTRW, and the FPT statistics is not well understood. It is known that 1D quenched systems exhibit distinct behaviors of diffusion [14,22].

Hence, filling the lacuna on the FPT statistics in 1D systems is critical to update fundamental understanding of diffusion in the quenched potential.

In this paper, we clarify several properties of the FPT statistics inherent to the quenched potential by looking at the 1D biased QTM. We first consider a periodic random potential and derive exact FPT statistics. We next show that the formulas are available to understand the nonperiodic potential also. Although the periodic potential landscape is employed to simplify the setup in this paper, stochastic dynamics in the periodic potential have been intensively studied analytically [23,24] and experimentally [25–28]. Moreover, a bias in diffusion processes induces surprising phenomena such as giant acceleration of diffusivity in periodic potentials [23,25], field-induced superdiffusion [29–32], and distinct initial ensemble dependence of diffusivity in disordered media such as the CTRW [33,34]. Our analysis also unravels several indications of the effects caused by quenched disorder on these phenomena.

II. MODEL AND MAIN RESULTS

We consider effects of bias on the FPT statistics in a quenched heterogeneous environment. In particular, we use a biased RW on a 1D quenched random energy landscape, which is periodically arranged, i.e., a biased QTM with a periodic landscape [see Fig. 1(a)] [22]. The target is located only at site L while the energy landscape is periodic. Probabilities of the right and left jumps are given by p and $q = 1 - p$, respectively. A biased RW implies $p \neq 1/2$, and here we consider $p > 1/2$. We assume that the tops of the

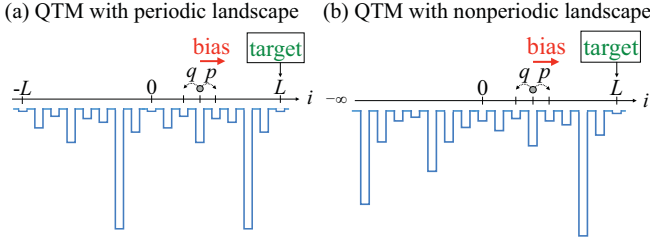(a) QTM with periodic landscape   (b) QTM with nonperiodic landscape

FIG. 1. Schematic representation of a biased QTM, where we represent a random energy landscape as a 1D energy landscape (a) with period L ($L = 8$) and (b) without periodicity. When a particle escapes from a valley of a random potential, it jumps to the right valley with probability p. A particle starts at the origin, and the target is located at site L. Note that there is no target on the left-hand side (no target at $0, -L, -2L, \ldots$). In other words, we consider a time when a particle makes a directed (clockwise or counterclockwise) revolution on a ring.

potentials are flat; i.e., the tops are the same height, implying that probability p does not affect the shape of the random energy landscape. This physical situation is relevant to a biased diffusion in heterogeneous comblike structures [35], e.g., porous media [31] and neuronal dendrites [36,37], in which the bias is considered to be a flow in the backbone.

We assume that the lattice constant is set to unity and number L of lattice sites with different energies is finite ($L < \infty$). At each site, depth E (> 0) of the energy trap is randomly assigned. In particular, the depths are independent and identically distributed (IID) random variables with an exponential distribution, $\rho(E) = T_g^{-1} \exp(-E/T_g)$, where T_g is called the glass temperature. A particle can escape from a trap and jump to one of the nearest neighbors. A waiting time when a particle escapes from the ith trap is a random variable, and the distribution follows the exponential distribution with mean τ_i: $\psi^{(i)}(\tau) = \tau_i^{-1} e^{-\tau/\tau_i}$ [38]. Mean waiting time τ_i follows the Arrhenius law, $\tau_i \propto \exp(E_i/T)$, where E_i is the depth of the energy at the ith trap and T denotes the temperature. Through the Arrhenius law and the energy distribution $\rho(E)$, the probability density function of τ_i follows a power law, $\psi_\alpha(\tau) \propto \tau^{-1-\alpha}$ with $\alpha \equiv T/T_g$ [39]. When the temperature is below T_g, $\alpha < 1$, the mean of τ_i diverges, inducing anomalous features such as anomalous diffusion and aging [14,22,40]. Note that sample mean waiting time

$$\mu_L = \frac{1}{L} \sum_{i=0}^{L-1} \tau_i \tag{1}$$

for a fixed disorder in the QTM with a periodic landscape never diverges when $L < \infty$.

We consider the FPT, i.e., a time when a particle starting from the origin reaches the target (site L) for the first time. As the main results of this study, we show the mean FPT (MFPT) and the variance of the FPT (VFPT) for a given quenched periodic landscape for large L:

$$\langle T \rangle_L \sim \frac{L\mu_L}{p - q} \equiv T_{\text{MFPT}}, \tag{2}$$

$$\langle \delta T^2 \rangle_L \sim \frac{L\{\sigma_L^2(p-q) + \mu_L^2\}}{(p-q)^3} \equiv T_{\text{VFPT}}, \tag{3}$$

where $\delta T \equiv T - \langle T \rangle_L$ and σ_L^2 is the sample variance:

$$\sigma_L^2 = \frac{1}{L} \sum_{i=0}^{L-1} \tau_i^2 - \mu_L^2. \tag{4}$$

Sample variance σ_L^2 quantifies the degree of heterogeneity. The VFPT for $\alpha < 1$ becomes $\langle \delta T^2 \rangle_L \sim L(\sigma_L^2 + \mu_L^2)/(p-q)^2$ because $\mu_L^2 = o(\sigma_L^2)$ for large L. In this paper, we discuss the physics behind the exact results and provide a brief sketch of the derivation. We note that the MFPT diverges when $p = q$ because the mean return time to the origin diverges. Therefore, the results include the case $p = q$. When the bias is small, $p - q$ can be expressed as $p - q \cong F/T$, where F is an external field. In this situation, the leading orders for small F dependencies of the FPT statistics are represented as $\langle T \rangle_L \propto 1/F$ and $\langle \delta T^2 \rangle_L \propto 1/F^3$.

A crucial aspect of the FPT statistics is that they are expressed by the statistics of the waiting times in the quenched heterogeneous environment. Note that the results do not explicitly include parameter α. Instead, they depend on μ_L and σ_L, which are finite and depend on each realization of the disorder. In addition, the VFPT are connected to the diffusivity in the biased QTM on a ring [23]. Therefore, the results play a significant role in estimating diffusivity, as discussed later.

The comparison of properties of FPTs in the QTM with those in the CTRW is intriguing. In the CTRW the waiting-time distribution is identical for all sites. Although the FPT distribution in CTRW has already been studied [20], the explicit forms of the FPT statistics have never been obtained so far. Importantly, our results also lead to the exact expressions of the biased CTRW (see the Appendices), which are given by

$$\langle T_{\text{ctrw}} \rangle_L \sim \frac{L\mu}{p - q}, \tag{5}$$

$$\langle \delta T_{\text{ctrw}}^2 \rangle_L \sim \frac{L\{\sigma^2(p-q)^2 + 4pq\mu^2\}}{(p-q)^3}, \tag{6}$$

where μ and σ^2 are the mean and the variance of the waiting-time distribution. The MFPT and VFPT diverge for $\alpha < 1$ and $\alpha < 2$, respectively, while the QTM results are finite for all regimes of α. The VFPT of the biased-CTRW is not given by a straightforward extension obtained from that of the biased QTM. This is unexpected because the CTRW is believed to be a good approximation of the QTM when a bias is added.

III. SAMPLE-TO-SAMPLE FLUCTUATIONS

We present numerical verifications of exact results (2) and (3) to see how these formulas work for each disorder realization. Figure 2 shows the MFPT and VFPT for 100 disorder realizations, where the numerical values are plotted as a function of the theoretical values. All the results are collapsed on the $y = x$ line, which shows a perfect agreement between the theory and numerical results. Note that the numerical results are provided for parameter $\alpha = 0.5$, where the disorder realizations show large sample-to-sample fluctuations. The MFPT and VFPT also exhibit strong sample-to-sample fluctuations because the disorder strongly affects μ_L and σ_L^2. Nevertheless, the theoretical values for different realizations are remarkably correct.
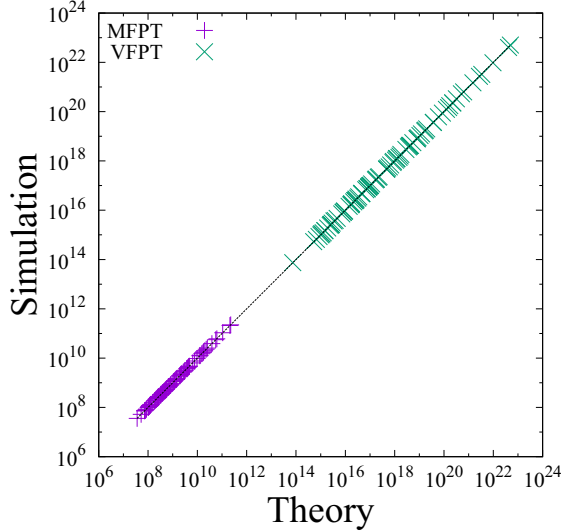
FIG. 2. Correlation plot for the MFPT and VFPT in the QTMs with periodic landscapes ($\alpha = 0.5$ and $L = 10^4$). Symbols represent results of numerical simulations for 100 different disorder realizations.

FIG. 3. (a) Ratio $\eta_{\nu,\varepsilon}$ as a function of L/N_{dis} ($N_{\text{dis}} = 10^3$, $\varepsilon = 0.5$, and $p = 0.8$) for nonperiodic landscapes. Symbols represent results of numerical simulations. We used 10^4 thermal paths to calculate the MFPT or VFPT for a fixed disorder realization. (b) Correlation plot for the MFPT and VFPT in the infinite 1D systems with nonperiodic landscapes ($\alpha = 0.5$ and $L = 10^3$). Numerical simulations of the MFPT and VFPT for 10^3 disorder realizations are presented by symbols.

Next, we discuss sample-to-sample fluctuations by considering a disorder average. In general, when the heterogeneity of a disorder realization is sufficiently weak, physical observables comprise self-averaging (SA) properties [22]. Here we quantify sample-to-sample fluctuations by the SA parameters defined as

$$\text{SA}(L; \langle \mathcal{O} \rangle_L) \equiv \frac{\langle \langle \mathcal{O} \rangle_L^2 \rangle_{\text{dis}} - \langle \langle \mathcal{O} \rangle_L \rangle_{\text{dis}}^2}{\langle \langle \mathcal{O} \rangle_L \rangle_{\text{dis}}^2}, \qquad (7)$$

where $\langle \cdot \rangle_{\text{dis}}$ indicates the disorder average and observable $\mathcal{O}$ is T or δT^2. The vanishing of these quantities implies a perfect realization of SA, and hence these parameters systematically quantify a degree of the SA property. This definition is analogous to that of the diffusivity in the QTM discussed in Ref. [41].

As μ_L is a random variable, the SA parameter for the MFPT, $\mathcal{O} = T$, can be rewritten as

$$\text{SA}(L; \langle T \rangle_L) = \frac{\langle \mu_L^2 \rangle_{\text{dis}} - \langle \mu_L \rangle_{\text{dis}}^2}{\langle \mu_L \rangle_{\text{dis}}^2} = \frac{\langle \tau^2 \rangle_{\text{dis}} - \langle \tau \rangle_{\text{dis}}^2}{L \langle \tau \rangle_{\text{dis}}^2}.$$

For $\alpha < 2$, the SA parameter is infinite because $\langle \tau^2 \rangle_{\text{dis}}$ diverges, while for $\alpha > 2$, it vanishes in the large-L limit, implying that the SA is satisfied for $\alpha > 2$, while it is violated for $\alpha < 2$. Hence, the transition between SA and non-SA occurs at $\alpha_c = 2$ for quantity $\langle T \rangle_L$. Similarly, the transition from SA to non-SA for quantity $\langle \delta T^2 \rangle_L$ can be discussed through Eq. (7). From a similar calculation, the critical value can be easily obtained as $\alpha_c = 4$; that is, the VFPT has an SA property for $\alpha > 4$, while it is broken for $\alpha < 4$.

IV. NUMERICAL ARGUMENT OF THE BIASED QTM WITH NONPERIODIC LANDSCAPE

We discuss the FPT statistics in the biased QTM in which the potentials are arranged randomly in the infinite line
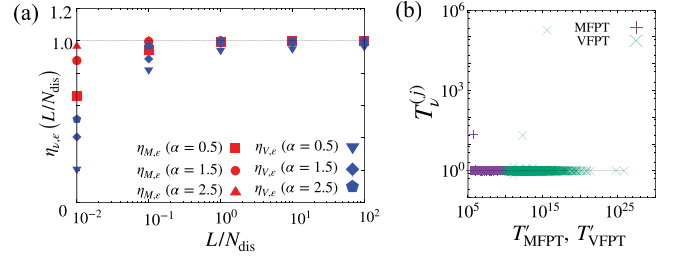
[Fig. 1(b)]. For a finite bias and large L, a particle will experience deep potentials mainly in the positive regime $i > 0$. Therefore, the FPT might be dominated by waiting times for regime $i > 0$. If this is true, the exact results for the periodic QTM may still be useful to understand the FPT statistics in the infinite 1D systems. To discuss the validity of this theory, we define the following two quantities:

$$T_{\text{M}} \equiv \frac{\langle T \rangle_L}{T'_{\text{MFPT}}} \quad \text{and} \quad T_{\text{V}} \equiv \frac{\langle \delta T^2 \rangle_L}{T'_{\text{VFPT}}}, \qquad (8)$$

where T'_{MFPT} and T'_{VFPT} are the same expressions as in Eqs. (2) and (3), respectively. We should note that μ_L and σ_L^2 in these expressions are calculated from τ_i for $i = 0, \ldots, L - 1$ (in other words, we do not use the information of potentials for $i < 0$). In addition, to quantify how our prediction works well, we introduce the following ratio:

$$\eta_{\nu,\varepsilon}\left(\frac{L}{N_{\text{dis}}}\right) \equiv \frac{1}{N_{\text{dis}}} \sum_{j=1}^{N_{\text{dis}}} I_{[1-\varepsilon, 1+\varepsilon]}\left(T_\nu^{(j)}\right), \quad \nu = \text{M, V}, \qquad (9)$$

where $T_\nu^{(j)}$ is a numerical value of T_ν for the jth realization of disorder and $I_A(x)$ is an indicator function, i.e., $I_A(x) = 1$ if $x \in A$ and $I_A(x) = 0$ otherwise. This quantifies a ratio that $T_\nu^{(j)}$ is within the corresponding theory with a ε-dependent accuracy. As shown in Fig. 3(a), the ratio approaches 1 with increasing L.

To understand more details at the level of each disorder realization, we next consider each $T_\nu^{(j)}$. In Fig. 3(b) we present numerical data of $T_\nu^{(j)}$ as a function of T'_{MFPT} or T'_{VFPT} depending on $\nu = \text{M}$ or V, respectively. Figure 3(b) shows that T'_{MFPT} and T'_{VFPT} are very good approximations of $\langle T \rangle_L$ and $\langle \delta T^2 \rangle_L$ for almost all realizations, except for a small number of realizations with extremely large deviations. In such rare samples, significantly large waiting times are assigned for $i < 0$ and small $|i|$ (see the Appendices). Except for such rare samples, the biased-QTM results with a periodic landscape are surprisingly useful in nonperiodic landscapes.

V. DERIVATION OF MAIN RESULTS

We now briefly describe the derivation of our results. We divide our explanation into two steps: step 1 explains the FPT in the standard biased RW (without random traps), and step 2 explains the FPT in the biased QTMs with periodic landscapes.

A. Step 1: Statistics of the numbers of visits

In the first step, we outline our main strategy to derive the main results for the QTM, which gives us another derivation for known results of the FPT statistics in the classical RW. The main strategy is to use statistics of the number of visits at each site. A similar quantity has also been employed to study diffusion of nonbiased motions [22,42]. A biased RW was studied in the context of the classical ruin problems [43]. In the ruin problems, a gambler with a capital wins or loses a dollar with probabilities p or q, respectively. The FPT from the origin to L site in the RW, i.e., $T_{\rm rw}$, correspond to a duration of the game in the ruin problems, in which the game is over when one of the two players is ruined. Here we consider that one of the players has infinite capital and his win probability is $p > 1/2$. The generating function for the FPT in the classical ruin problems was derived in Ref. [43], and the MFPT and VFPT are, respectively, obtained as

$$\langle T_{\rm rw}\rangle_L = \frac{L}{p-q} \quad \text{and} \quad \langle \delta T_{\rm rw}^2\rangle_L = \frac{4pqL}{(p-q)^3}. \quad (10)$$

While these results are exact for any L, we will consider the large-L limit to derive the biased-QTM results. Note that $\langle T_{\rm rw}\rangle$ is a special case of Eq. (2), while $\langle \delta T_{\rm rw}^2\rangle_L$ is not a special case of Eq. (3) [see Eq. (18) for the general result, which reproduces $\langle \delta T_{\rm rw}^2\rangle_L$].

The FPT from the origin to L site can be represented by the sum of the numbers of visits at each site,

$$T_{\rm rw} = \sum_{i=0}^{L-1} k_i, \quad (11)$$

where k_i is the number of visits to the ith site until the particle reaches site L. Note that k_i includes the number of the visits at sites $+i - nL$ ($n = 1, 2, \ldots$). To obtain the moments and correlation function of k_i, we consider the large-L limit. In this limit, the probability that a particle reaches site $-L$ becomes zero; i.e., a particle never visits the site $-L$. In the large-L limit, one can obtain the generating function of k_i until the particle reaches site L (see Appendix A):

$$Z(\lambda) \to \frac{p-q}{e^{-\lambda} - 2q}, \quad (12)$$

which yields the following:

$$\langle k_i\rangle \sim 1/(p-q) \quad \text{and} \quad \langle k_i^2\rangle - \langle k_i\rangle^2 \sim 2q/(p-q)^2 \quad (13)$$

for $L \to \infty$. Moreover, correlation $\langle k_i k_j\rangle$ can be obtained exactly as follows:

$$C_l \equiv \langle k_i k_{i+l}\rangle - \langle k\rangle^2 \to \frac{\varepsilon^l}{(p-q)^2} \quad (L \to \infty), \quad (14)$$

where $\varepsilon = q/p$, $\langle k\rangle = 1/(p-q)$, and $l \equiv |i - j|$. This correlation is derived in Appendix B. Note that C_l does not depend on i, and l is an arbitrary integer satisfying $l < L - i$.

The MFPT and second moment of the FPT can be, respectively, represented as

$$\langle T_{\rm rw}\rangle_L \sim L\langle k\rangle \quad \text{and} \quad \langle T_{\rm rw}^2\rangle_L \sim L(\langle \delta k^2\rangle + \langle k\rangle^2) + \sum_{i\neq j}\langle k_i k_j\rangle,$$

where $\langle \delta k^2\rangle = 2q/(p-q)^2$. Thus, the VFPT becomes

$$\langle \delta T_{\rm rw}^2\rangle_L = L\langle \delta k^2\rangle + 2\sum_{l=1}^{L-1}(L-l)C_l \sim L(\langle \delta k^2\rangle + 2C), \quad (15)$$

where $C = \sum_{l=1}^{L-1} C_l$. Note that $\sum_{l=1}^{L-1} lC_l$ converges to a constant for $L \to \infty$ because C_l decays exponentially to zero. In the large-L limit, we have

$$C = \frac{q}{(p-q)^3}. \quad (16)$$

This leads to the desired results of the MFPT and VFPT. Note that the RW results of the FPT statistics are exact for any L [43].

B. Step 2: Derivation of the QTM results

By using the same technique used in step 1, the biased-QTM results can be derived. Note that the FPT in the QTM can be obtained by

$$T = \sum_{i=0}^{L-1} T_i \quad \text{with} \quad T_i = \sum_{l=1}^{k_i} \tau_m^{(i)}, \quad (17)$$

where $\tau_m^{(i)}$ is the waiting time for the mth visit to site i and T_i is the occupation time at site i. The mean of T_i can be calculated as $\langle T_i\rangle = \langle \tau_1^{(i)} + \cdots + \tau_{k_i}^{(i)}\rangle = \langle k\rangle\tau_i$. Thus, the MFPT in the large-L limit is given by $\langle T\rangle_L \sim \langle k\rangle \sum_{i=0}^{L-1} \tau_i \sim L\mu_L/(p-q)$, i.e., Eq. (2). This is a simple extension of the MFPT for a biased RW and is easily obtained by multiplying $\langle T_{\rm rw}\rangle_L$ by μ_L.

Using $\langle T_i^2\rangle$, we also have the VFPT in the biased QTM (the details are given in Appendix C). In the large-L limit, the VFPT for $\alpha > 1$ becomes

$$\frac{\langle \delta T^2\rangle_L}{L} \sim \frac{2q(\sigma_L^2 + \mu_L^2)}{(p-q)^2} + \frac{\langle \delta\tau^2\rangle_L}{p-q} + \frac{2q\mu_L^2}{(p-q)^3}, \quad (18)$$

where

$$\langle \delta\tau^2\rangle_L = \frac{1}{L}\sum_{i=0}^{L-1}\left[\langle(\tau_l^{(i)})^2\rangle - \langle\tau_l^{(i)}\rangle^2\right]. \quad (19)$$

For $\alpha < 1$, μ_L^2 can be ignored because $\mu_L^2 = o(\sigma_L^2)$. In the QTM, $\langle \delta\tau^2\rangle_L = \sigma_L^2 + \mu_L^2$, which gives our main claim, Eq. (3). Note that Eq. (18) is a more general expression of the VFPT than Eq. (3), which includes the VFPT in the classical RW, $\langle \delta T_{\rm rw}^2\rangle_L$. Moreover, it is straightforward to derive exact results for the biased CTRW. In the CTRW, the waiting-time distribution is identical for all sites. Thus, sample variance σ_L^2 in CTRWs is zero. Replacing μ_L and $\langle \delta\tau^2\rangle_L$ with μ and σ^2 gives the exact expressions (5) and (6).

VI. DISCUSSION

We derived the MFPT and VFPT in the QTM with a random periodic potential in the presence of bias. In the large-L limit, our formulas provide the exact expressions of the FPT statistics in the biased CTRW. Unexpectedly, the VFPT values of the biased CTRW and QTM are distinctive. Furthermore, the results for the biased QTMs with periodic landscapes are still surprisingly useful even when the energy landscape is not periodically arranged in the 1D line.

Finally, we briefly discuss the diffusion coefficient in the biased QTM on a ring. Here we apply our formulas to diffusion in the system with period L. Let n_t be the number of events in which a particle makes a directed revolution (biased direction). As the time intervals between the events are IID random variables, the process of n_t is described as a renewal process. By renewal theory [44], the mean of n_t is given by $\langle n_t \rangle = t/\langle T \rangle_L$. Displacement δx_t is represented by $\delta x_t = L n_t + C_L$, where C_L is a random variable, and the mean has the order of L, $\langle C_L \rangle = O(L)$. Thus, $\langle \delta x_t \rangle$ becomes

$$\langle \delta x_t \rangle \sim L \langle n_t \rangle = \frac{(p-q)t}{\mu_L} \quad (t \to \infty). \tag{20}$$

Moreover, using the variance of n_t [44], we have

$$\langle \delta x_t^2 \rangle - \langle \delta x_t \rangle^2 \sim \left[\frac{(p-q)\big(\sigma_L^2 + \mu_L^2\big)}{\mu_L^3} + \frac{2q}{\mu_L} \right] t. \tag{21}$$

ACKNOWLEDGMENTS

APPENDIX A: DETAILS FOR A BIASED RANDOM WALK

A biased RW was studied in the context of the classical ruin problems [43] in which a gambler with a finite or infinite capital wins or loses a dollar with probabilities p and q, respectively. Let us consider the probability of his ruin when the initial capital is z and the other player's capital is $L - z$. In the language of the RW, this probability corresponds to the probability that a particle starting from site z ($0 \leqslant z \leqslant L$) reaches site 0 without visiting site L. This probability denoted by q_z^L is known as [43]

$$q_z^L = \frac{\varepsilon^L - \varepsilon^z}{\varepsilon^L - 1}, \tag{A1}$$

where $\varepsilon = q/p$. Moreover, the probability of his win is given by $p_z^L = 1 - q_z^L$ because the game will end in the future with probability 1.

Here we assume $p > 1/2$ and the random walker starts at the origin. The FPT from the origin to L site can be represented by the sum of the numbers of the visits at each site,

$$T_{\text{rw}} = \sum_{i=0}^{L-1} k_i, \tag{A2}$$

where k_i is the number of visits to the ith site until the particle reaches the site L. We note that k_i includes the number of the visits at sites $+i - nL$ ($n = 1, 2, \dots$).

To obtain the moments and the correlation function of k_i, we consider the large-L limit. In this limit, the probability that a particle starting at site -1 reaches site $-L$ is zero: $q_{L-1}^L \to 0$ for $L \to \infty$. Thus, a particle never visits site $-L$. This follows that the probability that a random walker visits site i ($n+1$)th times is given by

$$S(n) \sim p_{L-i}^L \sum_{k=0}^{n} {}_nC_k \big(pq_1^{L-i}\big)^k \big(qp_{L-1}^L\big)^{n-k} pp_1^{L-i}$$

$$= p_{L-i}^L \big(pq_1^{L-i} + qp_{L-1}^L\big)^n pp_1^{L-i} \tag{A3}$$

for $i \ll L$ because $q_{L-i}^L \to 0$ for $i \ll L$, and

$$S(n) \sim q_{L-i}^L \sum_{k=0}^{n-1} \big(pq_1^L + qp_{L-1}^L\big)^k pp_1^L \big(pq_1^{L-i} + qp_{L-1}^L\big)^{n-k-1}$$

$$\times pp_1^{L-i} + p_{L-i}^L \big(pq_1^{L-i} + qp_{L-1}^L\big)^n pp_1^{L-i} \tag{A4}$$

for $i \sim L$. In the large-L limit,

$$S(n) \to (p-q)(2q)^n \quad (L \to \infty), \tag{A5}$$

for both cases $i \ll L$ and $i \sim L$. Therefore, the generating function of the number of visits at site i until the particle reaches site L is given by

$$Z(\lambda) = \sum_{n=0}^{\infty} S(n) e^{\lambda(n+1)} \to \frac{p-q}{e^{-\lambda} - 2q} \tag{A6}$$

in the large-L limit. The generating function does not comprise i-dependence; that is, the distribution of k_i is the same for all i. Thus, the moments of k_i do not depend on the site. In particular, the mean and variance of k_i are given by

$$\langle k_i \rangle = \left. \frac{\partial Z(\lambda)}{\partial \lambda} \right|_{\lambda=0} = \frac{1}{p-q} \tag{A7}$$

and

$$\langle k_i^2 \rangle - \langle k_i \rangle^2 = \left. \frac{\partial^2 \ln Z(\lambda)}{\partial \lambda^2} \right|_{\lambda=0} = \frac{2q}{(p-q)^2}, \tag{A8}$$

respectively. Because the moments do not depend on site i, we use the following notations: $\langle k \rangle = 1/(p-q)$ and $\langle \delta k^2 \rangle = 2q/(p-q)^2$.

APPENDIX B: CORRELATION FUNCTION $\langle k_0 k_l \rangle$

To obtain correlation function $\langle k_0 k_l \rangle$, we consider the generating function defined by

$$Z(\lambda_0, \lambda_l) = \sum_{n_0, n_l} p(n_0, n_l) e^{\lambda_0 n_0} e^{\lambda_l n_l}, \tag{B1}$$

where $p(n_0, n_l)$ is the joint probability of $k_0 = n_0$ and $k_l = n_l$. Counting k_0 and k_l for $l > 1$, we have

$$Z(\lambda_0, \lambda_l) = \sum_{n_0=1}^{\infty} \left(q + pq_1^l + pp_1^l \sum_{k=1}^{\infty} \big\{P^{(l)}\big\}^{k-1} e^{k\lambda_l} qq_{l-1}^l \right)^{n_0-1}$$

$$\times e^{\lambda_0 n_0} pp_1^l \sum_{r=0}^{\infty} \{P^{(l)}\}^r e^{\lambda_l(r+1)} pp_1^{L-l}, \tag{B2}$$

where $P^{(l)}$ is the probability that a random walker starting from the site l will return to site l without visiting sites 0 and L, $P^{(l)} = pq_1^{L-l} + qp_{l-1}^l$. In the large-$L$ limit, the generating function becomes

$$Z(\lambda_0, \lambda_l) = \frac{e^{\lambda_0 + \lambda_l} pp_1^l(p-q)}{(1 - P^{(l)}e^{\lambda_l})[1 - (q + pq_1^l)e^{\lambda_0}] - pqq_{l-1}^l p_1^l e^{\lambda_0 + \lambda_l}}, \tag{B3}$$

which satisfies the normalization, $Z(0,0) = 1$.

The correlation function is given by

$$\langle k_0 k_l \rangle = \left. \frac{\partial^2 Z}{\partial \lambda_0 \lambda_l} \right|_{\lambda_0 = \lambda_l = 0} = \frac{1}{(p-q)^2} + \frac{\varepsilon^l}{(p-q)^2}, \tag{B4}$$

where $\varepsilon \equiv q/p < 1$. Thus, the correlation function decays exponentially. We note that this expression is valid for $l = 1$ because $q_0^1 = p_1^1 = 1$ and $p_0^1 = 0$.

Next, we consider $\langle k_i k_{i+l} \rangle$. Because the probability that a random walker starting from the origin visits site $-L + i + l$ for $i + l \ll L$ becomes zero in the large-L limit, for $i + l \ll L$ the generating function $Z(\lambda_i, \lambda_{i+l})$ is given by

$$Z(\lambda_i, \lambda_{i+l}) = \sum_{n_i=1}^{\infty} \left(q + pq_1^l + pp_1^l \sum_{k=1}^{\infty} \{P_i^{(l)}\}^{k-1} e^{k\lambda_{i+l}} qq_{l-1}^l \right)^{n_i-1} e^{\lambda_i n_i} pp_1^l \sum_{r=0}^{\infty} \{P_i^{(l)}\}^r e^{\lambda_{i+l}(r+1)} pp_1^{L-i-l}, \tag{B5}$$

where $P_i^{(l)} = pq_1^{L-i-l} + qp_{l-1}^l$, which is equivalent to $P^{(l)}$ in the large-L limit. Moreover, $p_1^{L-i-l} = p_1^{L-l}$ in the large-L limit. Therefore, $Z(\lambda_i, \lambda_{i+l})$ is the same as $Z(\lambda_0, \lambda_l)$ in the large-L limit. It follows that correlation function $\langle k_i k_{i+l} \rangle$ does not depend on i and is the same as $\langle k_0 k_l \rangle$.

For $i \sim L$, a random walker will visit site $-L + i + l$ with probability q_{L-i-l}^{L-l}, which is nonzero even in the large-L limit. Thus, the generating function becomes

$$Z(\lambda_i, \lambda_{i+l}) = q_{L-i-l}^{L-l} \sum_{n_{i+l}=1}^{\infty} \left(pq_1^{L-l} + qp_{l-1}^l + qq_{l-1}^l \sum_{k=1}^{\infty} \{P_{-L+i}\}^{k-1} e^{k\lambda_i} pp_1^l \right)^{n_{i+l}-1} e^{\lambda_{i+l} n_{i+l}}$$

$$\times pp_1^{L-l} \sum_{n_i=1}^{\infty} \left(q + pq_1^l + pp_1^l \sum_{k=1}^{\infty} \{P_i^{(l)}\}^{k-1} e^{k\lambda_{i+l}} qq_{l-1}^l \right)^{n_i-1} e^{\lambda_i n_i} pp_1^l \sum_{r=0}^{\infty} \{P_i^{(l)}\}^r e^{\lambda_{i+l}(r+1)} pp_1^{L-i-l}$$

$$+ p_{L-i-l}^{L-l} \sum_{n_i=1}^{\infty} \left(q + pq_1^l + pp_1^l \sum_{k=1}^{\infty} \{P_i^{(l)}\}^{k-1} e^{k\lambda_{i+l}} qq_{l-1}^l \right)^{n_i-1} e^{\lambda_i n_i} pp_1^l \sum_{r=0}^{\infty} \{P_i^{(l)}\}^r e^{\lambda_{i+l}(r+1)} pp_1^{L-i-l}, \tag{B6}$$

where $P_{-L+i} = q + pq_1^l$ and $P_i^{(l)} = pq_1^{L-i-l} + qp_{l-1}^l$. By a straightforward calculation, we have

$$\langle k_i k_{i+l} \rangle = \left. \frac{\partial^2 Z}{\partial \lambda_i \lambda_{i+l}} \right|_{\lambda_i = \lambda_{i+l} = 0} = \frac{1}{(p-q)^2} + \frac{\varepsilon^l}{(p-q)^2}. \tag{B7}$$

Therefore, the correlation function does not depend on i.

APPENDIX C: DERIVATION OF THE VFPT IN THE BIASED QTM

The second moment of T_i can be calculated as $\langle T_i^2 \rangle = \langle (\tau_1^{(i)} + \cdots + \tau_{k_i}^{(i)})^2 \rangle = \langle k^2 \rangle \langle (\tau_l^{(i)}) \rangle^2 + \langle k \rangle (\langle (\tau_l^{(i)})^2 \rangle - \langle (\tau_l^{(i)}) \rangle^2)$, where $\langle k^2 \rangle = \langle \delta k^2 \rangle + \langle k \rangle^2$, and $\langle (\tau_l^{(i)})^2 \rangle = 2\tau_i^2$ when the waiting-time distribution is the exponential distribution. Therefore, the second moment of the FPT in the QTM can be represented as

$$\langle T^2 \rangle_L = \sum_{i=0}^{L-1} \langle T_i^2 \rangle + \sum_{i \neq j} \langle T_i T_j \rangle = \langle k^2 \rangle \sum_{i=0}^{L-1} \tau_i^2 + \langle k \rangle \langle \delta \tau^2 \rangle_L L$$

$$+ \sum_{i \neq j} \langle k_i k_j \rangle \tau_i \tau_j, \tag{C1}$$

where

$$\langle \delta \tau^2 \rangle_L = \frac{1}{L} \sum_{i=0}^{L-1} [\langle (\tau_l^{(i)})^2 \rangle - \langle (\tau_l^{(i)}) \rangle^2]. \tag{C2}$$

The third term is given by $\sum_{i \neq j} \langle k_i k_j \rangle \tau_i \tau_j = 2 \sum_{l=1}^{L-1} C_l \sum_{i=0}^{L-1-l} \tau_i \tau_{i+l} + \langle k \rangle^2 \sum_{i \neq j} \tau_i \tau_j = 2 \sum_{l=1}^{L-1} C_l \sum_{i=0}^{L-1-l} \tau_i \tau_{i+l} + \langle k \rangle^2 [(\sum_{i=0}^{L-1} \tau_i)^2 - \sum_{i=0}^{L-1} \tau_i^2]$, where we set $C_l \equiv \langle k_i k_{i+l} \rangle - \langle k \rangle^2$ because $\langle k_i k_{i+l} \rangle$ does not depend on i. Therefore, the second moment of the FPT becomes

$$\langle T^2 \rangle_L = \langle \delta k^2 \rangle \sum_{i=0}^{L-1} \tau_i^2 + \langle k \rangle \langle \delta \tau^2 \rangle_L L + 2 \sum_{l=1}^{L-1} C_l \sum_{i=0}^{L-1-l} \tau_i \tau_{i+l}$$

$$+ \frac{L^2 \mu_L^2}{(p-q)^2}. \tag{C3}$$

The combination of Eqs. (A7), (A8), and (E6) gives Eq. (18).

APPENDIX D: SOME DISTRIBUTION FUNCTIONS

Here we define the probability density functions (PDFs) of $\tau_i \tau_{i+1}$ and τ_i^2, where τ_i and τ_{i+1} are independent and identically distributed random variables with a power-law distribution of $\psi_\alpha(\tau) = \alpha \tau^{-1-\alpha}$ ($\tau \geqslant 1$). First, the probability that τ_i^2 is smaller than x is given by

$$\Pr(\tau^2 < x) = \Pr(\tau < \sqrt{x}) = 1 - x^{-\alpha/2}. \quad \text{(D1)}$$

Therefore, the PDF of τ_i^2 is given by $\psi_{\alpha/2}(x)$. Next, the probability that $\tau_i \tau_{i+1}$ is smaller than x is given by

$$\Pr(\tau_i \tau_{i+1} \leqslant x) = \int_1^x \psi_\alpha(y) \Pr(\tau \leqslant x/y) \, dy \quad \text{(D2)}$$

$$= 1 - \alpha x^{-\alpha} - \alpha x^{-\alpha} \ln x. \quad \text{(D3)}$$

Thus, the PDF $\psi_{\tau_i \tau_{i+1}}(x)$ of $\tau_i \tau_{i+1}$ becomes

$$\psi_{\tau_i \tau_{i+1}}(x) \propto x^{-1-\alpha} \ln x \quad (x \to \infty). \quad \text{(D4)}$$

APPENDIX E: ASYMPTOTES

Here we consider the asymptotic behavior of $\sum_{l=1}^{L-1} C_l \sum_{i=0}^{L-1-l} \tau_i \tau_{i+l}$. First, we show that $a_l(L) = \sum_{i=0}^{L-1-l} \tau_i \tau_{i+l}$ satisfies $a_1 \sim a_m$ for $m \ll L$ in the large-L limit. In the large-L limit,

$$a_1(L) - a_m(L) \sim \sum_{i=0}^{L-m-1} \tau_i \Delta \tau_{i,m}, \quad \text{(E1)}$$

where $\Delta \tau_{i,m} = \tau_{i+1} - \tau_{i+m}$. Because τ_i and $\Delta \tau_{i,m}$ are independent and $\sum_{i=0}^{L-m-1} \Delta \tau_{i,m}/L \to 0$ for $L \to \infty$, the order of $a_1(L) - a_m(L)$ is at most that of $\sum_{i=0}^{L-1} \tau_i$: $O(L^{1/\alpha+1})$. It follows that $a_1(L) - a_m(L) = o[a_1(L)]$ because the PDF of $\tau_i \tau_j$ follows

$$\psi(x) \propto x^{-1-\alpha} \ln x \quad (x \to \infty), \quad \text{(E2)}$$

where τ_i and τ_j are independent. Therefore, we have $a_1 \sim a_m$ for $m \ll L$ in the large-L limit.

Because C_l decays exponentially to zero and $a_1 \sim a_l$ for $l \ll L$, $\sum_{l=1}^{L-1} C_l a_l(L)$ can be approximated by

$$\sum_{l=1}^{L-1} C_l a_l(L) \sim \sum_{l=1}^{m} C_l a_l(L) \sim C a_1(L), \quad \text{(E3)}$$

where m is small and does not depend on L and $C \equiv \sum_{l=1}^{L-1} C_l$.

Next, we show $\mu_L^2 \sim a_1/L$ for $\alpha > 1$ in the large-L limit. Because the sum of $\mu_L - \tau_{i+1}$ is a small order of L,

$$\sum_{i=0}^{L-2} (\mu_L - \tau_{i+1}) \sim \tau_0,$$

we have

$$\mu_L^2 - \frac{a_1(L)}{L} \sim \frac{1}{L} \sum_{i=0}^{L-2} \tau_i (\mu_L - \tau_{i+1}). \quad \text{(E4)}$$

For $\alpha > 1$, $\mu_L^2 - a_1(L)/L$ becomes small (and is a small order of μ_L^2) because $\sum_{i=1}^{L} \tau_i \tau_{i+1}/L \cong \mu_L^2$ for large L. Because μ_L is a small order of a_1/L, we have $\mu_L^2 - a_1(L)/L = o(a_1(L)/L)$,

$$a_1 \sim L \mu_L^2 \quad (L \to \infty). \quad \text{(E5)}$$

For $\alpha > 1$,

$$\sum_{l=1}^{L-1} C_l a_l(L) \sim L \mu_L^2. \quad \text{(E6)}$$

For $\alpha < 1$, the generalized central limit theorem states that

$$\frac{\sum_{i=1}^{L} \tau_i \tau_{i+1}}{L^{1/\alpha}} \Rightarrow Y_\alpha, \quad \text{(E7)}$$

where $\Rightarrow$ implies the convergence in distribution and Y_α is a random variable with a stable distribution with index α and

$$\frac{\sum_{i=1}^{L} \tau_i^2}{L^{2/\alpha}} \Rightarrow Y_{\alpha/2}. \quad \text{(E8)}$$

Thus, $a_1(L)/\sigma_L^2 \to 0$ for $L \to \infty$. Therefore, both μ_L^2 and $a_l(L)$ are small orders of σ_L^2. Thus, these terms in Eq. (C1) can be ignored.

APPENDIX F: DISORDER AVERAGE AND CORRELATION PLOT FOR THE MFPT AND VFPT IN THE INFINITE 1D SYSTEMS WITH NONPERIODIC LANDSCAPES

To quantify the degree of the disorder average, we introduce a sample-number-dependent variance:

$$\sigma_\nu^2(N_{\text{dis}}) \equiv \sum_{j=1}^{N_{\text{dis}}} \frac{\left(T_\nu^{(j)}\right)^2}{N_{\text{dis}}} - \left(\sum_{j=1}^{N_{\text{dis}}} \frac{T_\nu^{(j)}}{N_{\text{dis}}}\right)^2, \quad \nu = \text{M, V,} \quad \text{(F1)}$$

where $T_\nu^{(j)}$ is a numerical value of T_ν for the jth realization of disorder. This quantifies sample-to-sample fluctuations of $T_\nu^{(j)}$ as a function of N_{dis}. With increasing N_{dis}, the average approaches the exact disorder average. From the indication of the CTRW results (5) and (6), the exact disorder averages of FPT statistics will diverge for small α. In Fig. 4 we show the N_{dis} dependence of $\sigma_\nu^2(N_{\text{dis}})$. The figure clearly shows that $\sigma_M^2(N_{\text{dis}})$ and $\sigma_V^2(N_{\text{dis}})$ become divergent behaviors for $\alpha < 1$ and $\alpha < 2$, respectively, as increasing N_{dis}.

Figure 5 presents numerical data of $\langle T \rangle_L$ and $\langle \delta T^2 \rangle_L$. Numerical results on the $y = x$ line imply that T'_{MFPT} and T'_{VFPT} are very good approximations of the MFPT and VFPT, respectively. However, a few realizations deviate from the $y = x$ line. This figure explicitly explains a mechanism of
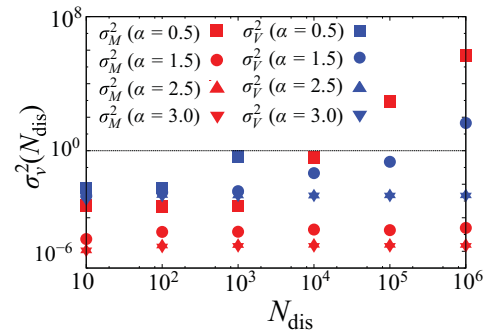

FIG. 4. Variances of T_M and T_V as a function of N_{dis} ($L = 10^3$ and $p = 0.8$). Symbols represent results of numerical simulations. We used 10^3 thermal paths to calculate the MFPT or VFPT for a fixed disorder realization.
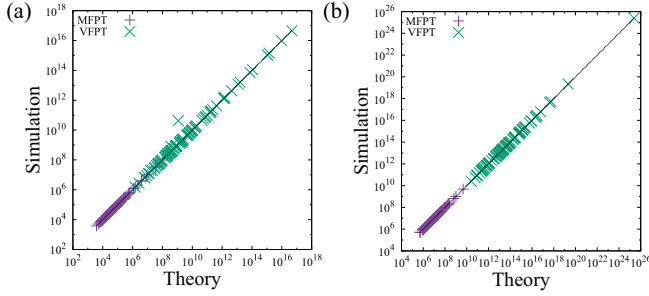
FIG. 5. Correlation plot for the MFPT and VFPT in the infinite 1D systems with nonperiodic landscapes ($\alpha = 0.5$) for (a) $L = 10^2$ and (b) $L = 10^3$. Numerical simulations of the MFPT and VFPT for 100 disorder realizations are presented by symbols. Some points deviate from the line, indicating the theories do not work well in these disorder realizations.

the divergence according to the disorder average; i.e., the divergence is caused by a small proportion of samples with extremely large deviations. In such rare samples, significantly large waiting times are assigned for $i < 0$ and small $|i|$. Except for such rare samples, the biased-QTM results with a periodic landscape are surprisingly useful in nonperiodic landscapes.

APPENDIX G: DERIVATION OF THE CTRW RESULTS

We derive the MFPT and VFPT in the CTRW following Ref. [20] and use the same notations as in Ref. [20] to present the MFPT as follows:

$$\langle T_{\text{ctrw}} \rangle_L = \int_0^\infty t \pi(t) \, dt = \sum_{n=1}^\infty Q(n) \int_0^\infty t \psi_n(t) \, dt. \quad (G1)$$

The Laplace transform of $\psi_n(t)$ can be given by $\hat{\psi}_n(s) = \hat{\psi}(s)^n$. It follows that

$$\int_0^\infty t \psi_n(t) \, dt = -n \hat{\psi}(0)^{n-1} \hat{\psi}'(0) = n\mu. \quad (G2)$$

Based on the classical RW result, we obtain

$$\langle T_{\text{ctrw}} \rangle_L = \mu \sum_{n=1}^\infty n Q(n) = \frac{\mu L}{p - q}. \quad (G3)$$

Similarly, we have

$$\langle T_{\text{ctrw}}^2 \rangle_L = \sum_{n=1}^\infty Q(n) \int_0^\infty t^2 \psi_n(t) \, dt \quad (G4)$$

$$= \sum_{n=1}^\infty Q(n)(n^2 \sigma^2 + n\mu^2) \quad (G5)$$

$$= \mu^2 \left[\frac{4pqL}{(p-q)^3} + \frac{L^2}{(p-q)^2} \right] + \frac{\sigma^2 L}{p-q}. \quad (G6)$$

Thus, the VFPT of the biased CTRW becomes Eq. (5).

[1] S. Redner, *A Guide to First-Passage Processes* (Cambridge University Press, Cambridge, 2001).

[2] O. G. Berg, R. B. Winter, and P. H. Von Hippel, Biochemistry **20**, 6929 (1981).

[3] P. H. von Hippel, Annu. Rev. Biophys. Biomol. Struct. **36**, 79 (2007).

[4] L. Mirny, Nat. Phys. **4**, 93 (2008).

[5] C. Loverdo, O. Bénichou, M. Moreau, and R. Voituriez, Nat. Phys. **4**, 134 (2008).

[6] L. Mirny, M. Slutsky, Z. Wunderlich, A. Tafvizi, J. Leith, and A. Kosmrlj, J. Phys. A **42**, 434013 (2009).

[7] M. A. Lomholt, B. van den Broek, S.-M. J. Kalisch, G. J. Wuite, and R. Metzler, Proc. Natl. Acad. Sci. USA **106**, 8204 (2009).

[8] O. Bénichou, C. Loverdo, M. Moreau, and R. Voituriez, Rev. Mod. Phys. **83**, 81 (2011).

[9] N. Shimamoto, J. Biol. Chem. **274**, 15293 (1999).

[10] W. Li and K. Kaneko, Europhys. Lett. **17**, 655 (1992).

[11] Y. M. Wang, R. H. Austin, and E. C. Cox, Phys. Rev. Lett. **97**, 048302 (2006).

[12] A. Granéli, C. C. Yeykal, R. B. Robertson, and E. C. Greene, Proc. Natl. Acad. Sci. USA **103**, 1221 (2006).

[13] Y. He, S. Burov, R. Metzler, and E. Barkai, Phys. Rev. Lett. **101**, 058101 (2008).

[14] T. Miyaguchi and T. Akimoto, Phys. Rev. E **83**, 031926 (2011); **91**, 010102(R) (2015).

[15] M. Slutsky, M. Kardar, and L. A. Mirny, Phys. Rev. E **69**, 061903 (2004).

[16] M. Slutsky and L. A. Mirny, Biophys. J. **87**, 4021 (2004).

[17] R. Zwanzig, Proc. Natl. Acad. Sci. USA **85**, 2029 (1988).

[18] G. Rangarajan and M. Ding, Phys. Lett. A **273**, 322 (2000).

[19] E. Barkai, Phys. Rev. E **63**, 046118 (2001).

[20] S. Condamin, O. Bénichou, and J. Klafter, Phys. Rev. Lett. **98**, 250602 (2007).

[21] H. Krüsemann, A. Godec, and R. Metzler, Phys. Rev. E **89**, 040101(R) (2014); J. Phys. A **48**, 285001 (2015).

[22] J. Bouchaud and A. Georges, Phys. Rep. **195**, 127 (1990).

[23] P. Reimann, C. Van den Broeck, H. Linke, P. Hänggi, J. M. Rubi, and A. Pérez-Madrid, Phys. Rev. Lett. **87**, 010602 (2001); Phys. Rev. E **65**, 031104 (2002).

[24] D. S. Dean, S. Gupta, G. Oshanin, A. Rosso, and G. Schehr, J. Phys. A **47**, 372001 (2014).

[25] P. Reimann and R. Eichhorn, Phys. Rev. Lett. **101**, 180601 (2008).

[26] R. Hayashi, K. Sasaki, S. Nakamura, S. Kudo, Y. Inoue, H. Noji, and K. Hayashi, Phys. Rev. Lett. **114**, 248101 (2015).

[27] X.-G. Ma, P.-Y. Lai, B. J. Ackerson, and P. Tong, Phys. Rev. E **91**, 042306 (2015); X.-G. Ma, Y. Su, P.-Y. Lai, and P. Tong, *ibid.* **96**, 012601 (2017).

[28] D. Kim, C. Bowman, J. T. Del Bonis-O'Donnell, A. Matzavinos, and D. Stein, Phys. Rev. Lett. **118**, 048002 (2017).

[29] M. F. Shlesinger, J. Stat. Phys. **10**, 421 (1974).

[30] G. Margolin and B. Berkowitz, Phys. Rev. E **65**, 031101 (2002).

[31] B. Berkowitz, A. Cortis, M. Dentz, and H. Scher, Rev. Geophys. **44**, RG2003 (2006).

[32] R. Burioni, G. Gradenigo, A. Sarracino, A. Vezzani, and A. Vulpiani, J. Stat. Mech. (2013) P09022; R. Burioni, G. Gradenigo, A. Sarracino, A. Vezzani, and A. Vulpiani, Commun. Theor. Phys. **62**, 514 (2014).

[33] T. Akimoto, A. G. Cherstvy, and R. Metzler, Phys. Rev. E **98**, 022105 (2018).

[34] R. Hou, A. G. Cherstvy, R. Metzler, and T. Akimoto, Phys. Chem. Chem. Phys. **20**, 20827 (2018).

[35] A. M. Berezhkovskii, L. Dagdug, and S. M. Bezrukov, J. Chem. Phys. **142**, 134101 (2015).

[36] V. Méndez and A. Iomin, Chaos Solitons Fractals **53**, 46 (2013).

[37] R. Jose, L. Santen, and M. R. Shaebani, Biophys. J. **115**, 2014 (2018).

[38] V. Mel'nikov, Phys. Rep. **209**, 1 (1991).

[39] F. Bardou, J.-P. Bouchaud, A. Aspect, and C. Cohen-Tannoudji, *Lévy Statistics and Laser Cooling: How Rare Events Bring Atoms to Rest* (Cambridge University Press, Cambridge, 2002); T. Akimoto, E. Barkai, and K. Saito, Phys. Rev. E **97**, 052143 (2018).

[40] E. M. Bertin and J.-P. Bouchaud, Phys. Rev. E **67**, 026128 (2003).

[41] T. Akimoto, E. Barkai, and K. Saito, Phys. Rev. Lett. **117**, 180602 (2016).

[42] S. Burov and E. Barkai, Phys. Rev. Lett. **106**, 140602 (2011).

[43] W. Feller, *An Introduction to Probability Theory and Its Applications* (John Wiley & Sons, New York, 1968), Vol. 1.

[44] D. R. Cox, *Renewal Theory* (Methuen, London, 1962).